

Piezoelectricity in wurtzite polar semiconductor nanowires: A theoretical study

Banani Sen, Michael Strosio, and Mitra Dutta

Citation: *J. Appl. Phys.* **110**, 024506 (2011); doi: 10.1063/1.3603036

View online: <http://dx.doi.org/10.1063/1.3603036>

View Table of Contents: <http://jap.aip.org/resource/1/JAPIAU/v110/i2>

Published by the [American Institute of Physics](#).

Related Articles

Growth-in-place deployment of in-plane silicon nanowires

Appl. Phys. Lett. **99**, 203104 (2011)

Vapor-liquid-solid and vapor-solid growth of self-catalyzed GaAs nanowires

AIP Advances **1**, 042142 (2011)

Study on transport pathway in oxide nanowire growth by using spacing-controlled regular array

Appl. Phys. Lett. **99**, 193105 (2011)

Facile fabrication of lateral nanowire wrap-gate devices with improved performance

Appl. Phys. Lett. **99**, 173101 (2011)

Why self-catalyzed nanowires are most suitable for large-scale hierarchical integrated designs of nanowire nanoelectronics

J. Appl. Phys. **110**, 084310 (2011)

Additional information on J. Appl. Phys.

Journal Homepage: <http://jap.aip.org/>

Journal Information: http://jap.aip.org/about/about_the_journal

Top downloads: http://jap.aip.org/features/most_downloaded

Information for Authors: <http://jap.aip.org/authors>

ADVERTISEMENT

AIPAdvances

Submit Now

**Explore AIP's new
open-access journal**

- **Article-level metrics
now available**
- **Join the conversation!
Rate & comment on articles**

Piezoelectricity in wurtzite polar semiconductor nanowires: A theoretical study

Banani Sen,^{a)} Michael Strosio,^{b)} and Mitra Dutta^{c)}

Department of Electrical and Computer Engineering, University of Illinois at Chicago, Chicago, Illinois 60607, USA

(Received 28 April 2011; accepted 22 May 2011; published online 22 July 2011)

By considering acoustic phonon mode displacements in nanowires, the piezoelectrically induced electric polarization vector and the associated potential are calculated. For the case of charge-free semiconductor nanowires, the piezo energies generated by strains applied in different directions are compared. For the directions considered, it is found that the maximum piezo energy in these nanowires is generated for strain applied in the vertical direction (i.e., along z-axis). Moreover, for these nanowires, energy generation in AlN and ZnO are found to be superior to GaN, just as expected based on past treatments of nanowires using phonons of bulk structures. © 2011 American Institute of Physics. [doi:10.1063/1.3603036]

I. INTRODUCTION

Energy harvesting has been around for centuries in the form of windmills, watermills, and passive solar power systems. Among the different forms of energy harvesting, vibration-based mechanical energy being the most ubiquitous and accessible energy source in the surroundings, harvesting this type of energy exhibits a great potential for remote or wireless sensing, charging batteries, and powering electronic devices. Over the last decade, much research has been focused on energy harvesting using piezoelectric semiconductor nanowires to harvest energy on the microscale and nanoscale.^{1,2} Owing to the small size and high flexibility of the nanowires, the nanogenerators are very sensitive to small level mechanical disturbances and are ideal for powering wireless sensors, microrobots, nano/micro electro-mechanical systems (NEMS/MEMS) and bioimplantable devices.^{3,4} Yet, the physics behind the electromechanical phenomena of these semiconductors is poorly studied. In this paper we have presented a detailed study of the electromechanical phenomena in light of the piezoelectric polarization of these materials.

The piezoelectric interaction occurs in all polar crystals lacking an inversion symmetry. On application of an external strain to a piezoelectric crystal, a macroscopic polarization is produced as a result of the displacements of ions. Thus, an acoustic phonon mode will drive a macroscopic polarization in a piezoelectric crystal. The polar crystals are generally of three types: the wurtzite, the zincblende and the rock salt. The wurtzites are the most stable and therefore most commonly considered at ambient conditions. The zinc blende form can be stabilized using substrates with cubic lattice structure and the rarely found rocksalt (NaCl-type) structure is only observed at relatively high pressures. In this paper we have restricted ourselves to the most common type, i.e., the hexagonal wurtzite structure.

II. THEORY

In order to determine the piezoelectric polarization in a wurtzite material, it is necessary to consider the piezoelectric tensor of the material under consideration and to determine the strain components corresponding to the deformation under consideration. The piezoelectric tensor relating the piezoelectric polarization vector and the acoustic strain vector may be expressed in matrix notation for the case of a wurtzite crystal in Cartesian coordinates as

$$\bar{e} = \begin{pmatrix} 0 & 0 & 0 & 0 & e_{x5} & 0 \\ 0 & 0 & 0 & e_{x5} & 0 & 0 \\ e_{z1} & e_{z1} & e_{z3} & 0 & 0 & 0 \end{pmatrix}. \quad (1)$$

For the case of uniform plane wave propagation at an arbitrary angle η in the XZ plane of a wurtzite crystal, the piezoelectric stress matrix transforms as

$$\bar{e}' = [a] [\bar{e}] [\tilde{M}], \quad (2)$$

where the rotation transformation matrix $[a]$ is given by

$$[a] = \begin{pmatrix} \cos \eta & 0 & -\sin \eta \\ 0 & 0 & 1 \\ \sin \eta & 0 & \cos \eta \end{pmatrix}$$

and the bond stress transformation matrix $[M]$ is derived from $[a]$.⁵

Therefore, the piezoelectric stress tensor \bar{e}' for propagation at an arbitrary angle η in the XZ plane of a wurtzite crystal is given by

$$\bar{e}' = \begin{pmatrix} e'_{x1} & e'_{x2} & e'_{x3} & 0 & e'_{x5} & 0 \\ 0 & 0 & 0 & e'_{y4} & 0 & e'_{y6} \\ e'_{z1} & e'_{z2} & e'_{z3} & 0 & e'_{z5} & 0 \end{pmatrix} \quad (3)$$

with

$$e'_{x1} = -e_{z1} \sin \eta \cos^2 \eta - e_{z3} \sin^3 \eta - e_{x5} \cos \eta \sin 2\eta,$$

$$e'_{x2} = -e_{z1} \sin \eta,$$

$$e'_{x3} = -e_{z1} \sin^3 \eta - e_{z3} \cos^2 \eta \sin \eta + e_{x5} \cos \eta \sin 2\eta[?],$$

$$e'_{x5} = -e_{z1} \frac{\sin \eta \sin 2\eta}{2} + e_{z3} \frac{\sin \eta \sin 2\eta}{2} + e_{x5} \cos \eta \cos 2\eta,$$

^{a)}Electronic mail: bananisen@iee.org.

^{b)}Also at Physics Department, University of Illinois at Chicago, Chicago, Illinois 60607, USA and Bioengineering Department, University of Illinois at Chicago, Illinois 60607, USA.

^{c)}Also at Physics Department, University of Illinois at Chicago, Chicago, Illinois 60607, USA.

$$\begin{aligned}
e'_{y4} &= e_{x5} \cos \eta, \\
e'_{y6} &= -e_{x5} \sin \eta, \\
e'_{z1} &= e_{z1} \cos^3 \eta + e_{z3} \cos \eta \sin^2 \eta - e_{x5} \sin \eta \sin 2\eta, \\
e'_{z2} &= e_{z1} \cos \eta, \\
e'_{z3} &= e_{z1} \cos \eta \sin^2 \eta + e_{z3} \cos^3 \eta + e_{x5} \sin \eta \sin 2\eta, \\
e'_{z5} &= e_{z1} \frac{\cos \eta \sin 2\eta}{2} - e_{z3} \frac{\cos \eta \sin 2\eta}{2} + e_{x5} \sin \eta \cos 2\eta.
\end{aligned}$$

In order to cast \bar{e}' into a more suitable form for cylindrical quantum wires, we made a transformation from the Cartesian coordinate system to the cylindrical coordinate system. In the cylindrical polar coordinate system, the piezoelectric stress tensor \bar{e}' for propagation at an angle η in the XZ plane of a wurtzite crystal transforms as

$$\bar{e}'' = [a'] [\bar{e}'] [\tilde{M}'], \quad (4)$$

where the coordinate transformation matrix $[a']$ is given by

$$[a'] = \begin{pmatrix} \cos \phi & \sin \phi & 0 \\ -\sin \phi & \cos \phi & 0 \\ 0 & 0 & 1 \end{pmatrix}$$

and the bond stress transformation matrix $[M']$ for this case is derived from $[a']$. Therefore, the piezoelectric stress tensor in cylindrical coordinates is given by

$$\bar{e}'' = \begin{pmatrix} e''_{x1} & e''_{x2} & e''_{x3} & e''_{x4} & e''_{x5} & e''_{x6} \\ e''_{y1} & e''_{y2} & e''_{y3} & e''_{y4} & e''_{y5} & e''_{y6} \\ e''_{z1} & e''_{z2} & e''_{z3} & e''_{z4} & e''_{z5} & e''_{z6} \end{pmatrix}, \quad (5)$$

with

$$\begin{aligned}
e''_{x1} &= e'_{x1} \cos^3 \phi + e'_{x2} \cos \phi \sin^2 \phi + e'_{y6} \sin \phi \sin 2\phi, \\
e''_{x2} &= e'_{x1} \cos \phi \sin^2 \phi + e'_{x2} \cos^3 \phi - e'_{y6} \sin \phi \sin 2\phi, \\
e''_{x3} &= e'_{x3} \cos \phi, \\
e''_{x4} &= e'_{y4} \sin \phi \cos \phi - e'_{x5} \sin \phi \cos \phi, \\
e''_{x5} &= e'_{y4} \sin^2 \phi + e'_{x5} \cos^2 \phi, \\
e''_{x6} &= -e'_{x1} \cos \phi \frac{\sin 2\phi}{2} + e'_{x2} \cos \phi \frac{\sin 2\phi}{2} \\
&\quad + e'_{y6} \sin \phi \cos 2\phi, \\
e''_{y1} &= -e'_{x1} \sin \phi \cos^2 \phi - e'_{x2} \sin \phi^3 \\
&\quad + e'_{y6} \cos \phi \sin 2\phi, \\
e''_{y2} &= -e'_{x1} \sin^3 \phi - e'_{x2} \sin \phi \cos^2 \phi - e'_{y6} \cos \phi \sin 2\phi, \\
e''_{y3} &= -e'_{x3} \sin \phi, \\
e''_{y4} &= e'_{y4} \cos^2 \phi + e'_{x5} \sin^2 \phi, \\
e''_{y5} &= e'_{y4} \sin \phi \cos \phi - e'_{x5} \sin \phi \cos \phi, \\
e''_{y6} &= e'_{x1} \sin \phi \frac{\sin 2\phi}{2} - e'_{x2} \sin \phi \frac{\sin 2\phi}{2} \\
&\quad + e'_{y6} \cos \phi \cos 2\phi, \\
e''_{z1} &= e'_{z1} \cos^2 \phi + e'_{z2} \sin^2 \phi, \\
e''_{z2} &= e'_{z1} \sin^2 \phi + e'_{z2} \cos^2 \phi, \\
e''_{z3} &= e'_{z3}, \\
e''_{z4} &= -e'_{z5} \sin \phi,
\end{aligned}$$

$$\begin{aligned}
e''_{z5} &= e'_{z5} \cos \phi, \\
e''_{z6} &= -e'_{z1} \frac{\sin 2\phi}{2} + e'_{z2} \frac{\sin 2\phi}{2}.
\end{aligned}$$

The piezoelectrically induced electric polarization vector \bar{P} is given in terms of the piezoelectric tensor \bar{e}'' and the acoustic strain vector \bar{S} by the matrix equation

$$\bar{P} = \bar{e}'' \cdot \bar{S}, \quad (6)$$

where \bar{P} is a three-component vector and \bar{S} is the six-component strain vector as given below

$$\bar{P} = \begin{pmatrix} P_r \\ P_\phi \\ P_z \end{pmatrix}, \quad \bar{S} = \begin{pmatrix} S_{rr} \\ S_{\phi\phi} \\ S_{zz} \\ 2S_{z\phi} \\ 2S_{rz} \\ 2S_{r\phi} \end{pmatrix},$$

with the strain components

$$\begin{aligned}
S_{rr} &= \frac{1}{i\omega} \frac{\partial v_r}{\partial r} = \frac{\partial u_r}{\partial r}, \\
S_{\phi\phi} &= \frac{1}{i\omega} \left(\frac{v_r}{r} + \frac{1}{r} \frac{\partial v_\phi}{\partial \phi} \right) = \frac{u_r}{r} + \frac{1}{r} \frac{\partial u_\phi}{\partial \phi}, \\
S_{zz} &= \frac{1}{i\omega} \frac{\partial v_z}{\partial z} = \frac{\partial u_z}{\partial z}, \\
2S_{z\phi} &= \frac{1}{i\omega} \left(\frac{\partial v_\phi}{\partial z} + \frac{1}{r} \frac{\partial v_z}{\partial \phi} \right) = \frac{\partial u_\phi}{\partial z} + \frac{1}{r} \frac{\partial u_z}{\partial \phi}, \\
2S_{rz} &= \frac{1}{i\omega} \left(\frac{\partial v_r}{\partial z} + \frac{\partial v_z}{\partial r} \right) = \frac{\partial u_r}{\partial z} + \frac{\partial u_z}{\partial r}, \\
2S_{r\phi} &= \left(\frac{1}{r} \frac{\partial v_r}{\partial \phi} + \frac{\partial v_\phi}{\partial r} - \frac{v_\phi}{r} \right) = \frac{1}{r} \frac{\partial u_r}{\partial \phi} + \frac{\partial u_\phi}{\partial r} - \frac{u_\phi}{r}
\end{aligned}$$

with v being the velocity associated with the acoustic phonon displacement, u and ω being the harmonic frequency assumed for the phonon field, i.e., $v = i\omega u$.⁶

Therefore, the components of the piezoelectrically induced polarization tensor in cylindrical polar coordinate system are given by

$$\begin{aligned}
P_r &= (e'_{x1} \cos^3 \phi + e'_{x2} \cos \phi \sin^2 \phi + e'_{y6} \sin \phi \sin 2\phi) \frac{\partial u_r}{\partial r} \\
&\quad + (e'_{x1} \cos \phi \sin^2 \phi + e'_{x2} \cos^3 \phi - e'_{y6} \sin \phi \sin 2\phi) \\
&\quad \times \left(\frac{u_r}{r} + \frac{1}{r} \frac{\partial u_\phi}{\partial \phi} \right) + e'_{x3} \cos \phi \frac{\partial u_z}{\partial z} + (e'_{y4} \sin \phi \cos \phi \\
&\quad - e'_{x5} \cos \phi \sin \phi) \left(\frac{\partial u_\phi}{\partial z} + \frac{1}{r} \frac{\partial u_z}{\partial \phi} \right) + (e'_{y4} \sin^2 \phi + e'_{x5} \cos^2 \phi) \\
&\quad \times \left(\frac{\partial u_r}{\partial z} + \frac{\partial u_z}{\partial r} \right) + \left(-e'_{x1} \cos \phi \frac{\sin 2\phi}{2} + e'_{x2} \cos \phi \frac{\sin 2\phi}{2} \right. \\
&\quad \left. + e'_{y6} \sin \phi \cos 2\phi \right) \left(\frac{1}{r} \frac{\partial u_r}{\partial \phi} + \frac{\partial u_\phi}{\partial r} - \frac{u_\phi}{r} \right), \quad (7a)
\end{aligned}$$

$$\begin{aligned}
P_\phi = & (e'_{x1} \sin \phi \cos^2 \phi - e'_{x2} \sin^3 \phi + e'_{y6} \cos \phi \sin 2\phi) \frac{\partial u_r}{\partial r} - (e'_{x1} \sin^3 \phi + e'_{x2} \sin \phi \cos^2 \phi \\
& + e'_{y6} \cos \phi \sin 2\phi) \left(\frac{u_r}{r} + \frac{1}{r} \frac{\partial u_\phi}{\partial \phi} \right) - e'_{x3} \sin \phi \frac{\partial u_z}{\partial z} + (e'_{y4} \cos^2 \phi + e'_{x5} \sin^2 \phi) \left(\frac{\partial u_\phi}{\partial z} + \frac{1}{r} \frac{\partial u_z}{\partial \phi} \right) \\
& + (e'_{y4} \sin \phi \cos \phi - e'_{x5} \sin \phi \cos \phi) \left(\frac{\partial u_r}{\partial z} + \frac{\partial u_z}{\partial r} \right) + \left(e'_{x1} \sin \phi \frac{\sin 2\phi}{2} - e'_{x2} \sin \phi \frac{\sin 2\phi}{2} \right. \\
& \left. + e'_{y6} \cos \phi \cos 2\phi \right) \left(\frac{1}{r} \frac{\partial u_r}{\partial \phi} + \frac{\partial u_\phi}{\partial r} - \frac{u_\phi}{r} \right), \tag{7b}
\end{aligned}$$

$$\begin{aligned}
P_z = & (e'_{z1} \cos^2 \phi + e'_{z2} \sin^2 \phi) \frac{\partial u_r}{\partial r} + (e'_{z1} \sin^2 \phi + e'_{z2} \cos^2 \phi) \left(\frac{u_r}{r} + \frac{1}{r} \frac{\partial u_\phi}{\partial \phi} \right) + e'_{z3} \frac{\partial u_z}{\partial z} \\
& - e'_{z5} \sin \phi \left(\frac{\partial u_\phi}{\partial z} + \frac{1}{r} \frac{\partial u_z}{\partial \phi} \right) + e'_{z5} \cos \phi \left(\frac{\partial u_r}{\partial z} + \frac{\partial u_z}{\partial r} \right) + \left(-e'_{z1} \frac{\sin 2\phi}{2} + e'_{z2} \frac{\sin 2\phi}{2} \right) \\
& \times \left(\frac{1}{r} \frac{\partial u_r}{\partial \phi} + \frac{\partial u_\phi}{\partial r} - \frac{u_\phi}{r} \right) \tag{7c}
\end{aligned}$$

The static permittivity for a hexagonal wurtzite crystal is given as

$$\epsilon = \begin{pmatrix} \epsilon_{xx} & 0 & 0 \\ 0 & \epsilon_{xx} & 0 \\ 0 & 0 & \epsilon_{zz} \end{pmatrix}$$

Now for phonon propagation at an arbitrary angle η in the XZ plane, the permittivity matrix transforms as

$$\epsilon' = [a] [\epsilon] [\tilde{a}]. \tag{8}$$

Again, on coordinate transformation, the static permittivity transforms as

$$\epsilon'' = [a'] [\epsilon'] [\tilde{a}']. \tag{9}$$

In general the electric displacement vector is given by

$$\bar{D} = \epsilon_0 \bar{E} + \bar{P} = \epsilon \bar{E}. \tag{10}$$

Therefore for the case of no free charge in the nanowire, the piezoelectric potential generated in the nanowire due to the piezoelectric polarization is given by

$$V = -\frac{1}{\epsilon - \epsilon_0} \int \bar{P} \cdot d\bar{p} \tag{11}$$

$$= -\frac{1}{\epsilon'' - \epsilon_0} \left[\int P_r dr + \int r P_\phi d\phi + \int P_z dz \right]. \tag{12}$$

III. PIEZOELECTRIC STIFFENING

Another important phenomenon in piezoelectric materials is the piezoelectric stiffening. Piezoelectric stiffening is caused by the generation of an electric field from the strain applied and subsequent generation of piezoelectric stress in the piezoelectric materials. According to the Christoffel equation, the change in elastic stiffness (C) is a function of the piezoelectric constants, permittivity and the wave vector

direction (\bar{l}) and in matrix notation, the elastic stiffness tensor at zero electric displacement is given as

$$C^D = C_{KL}^E + \frac{[e_{Kj} l_j] [l_i e_{iL}]}{l_i \epsilon_{ij} l_j} \tag{13a}$$

$$= C_{KL}^E \left(1 + (K_{KL}(\bar{l}))^2 \right), \tag{13b}$$

where

$$(K_{KL}(\bar{l}))^2 = \frac{[e_{Kj} l_j] [l_i e_{iL}]}{(l_i \epsilon_{ij} l_j) (C_{KL}^E)} \tag{14}$$

often called as the electromechanical coupling constant.

The elastic stiffness tensor in matrix notation for the case of a wurtzite crystal in Cartesian coordinates is given as

$$C_{KL}^E = \begin{pmatrix} C_{11}^E & C_{12}^E & C_{13}^E & 0 & 0 & 0 \\ C_{12}^E & C_{11}^E & C_{13}^E & 0 & 0 & 0 \\ C_{13}^E & C_{13}^E & C_{33}^E & 0 & 0 & 0 \\ 0 & 0 & 0 & C_{44}^E & 0 & 0 \\ 0 & 0 & 0 & 0 & C_{44}^E & 0 \\ 0 & 0 & 0 & 0 & 0 & \frac{1}{2}(C_{11}^E - C_{12}^E) \end{pmatrix}. \tag{15}$$

For the case of uniform plane wave propagation at an arbitrary angle η in the XZ plane of a wurtzite crystal, the elastic stiffness matrix transforms as

$$C_{KL}^{E'} = [M] [C_{KL}^E] [\tilde{M}]. \tag{16}$$

Among the polar semiconductors, the group III nitrides such as AlN and GaN and the group II oxide, ZnO, are gaining more importance for energy related applications. The static dielectric constant (ϵ_0) and the piezoelectric constants (e_{ij}) and the elastic stiffness constants (C_{ij}^E) for these materials are given in Table I.

TABLE I. Static dielectric constants, piezoelectric coefficients, and elastic stiffness constants for AlN, ZnO, and GaN (wurtzite structure) from the literature.

| Material parameters | | AlN ^a | ZnO ^b | GaN ^c |
|---------------------|-----------------|------------------|------------------|------------------|
| E | $E \parallel c$ | 8.22 | 8.59 | 10.4 |
| | $E \perp c$ | 7.91 | 7.46 | 9.5 |
| $e_{ij}(C/m^2)$ | e_{x5} | -0.48 | -0.45 | -0.3 |
| | e_{z1} | -0.58 | -0.51 | -0.33 |
| | e_{z3} | 1.55 | 1.22 | 0.65 |
| $C_{ij}^E(GPa)$ | C_{11}^E | 411 | 210 | 296 |
| | C_{12}^E | 149 | 121 | 130 |
| | C_{13}^E | 99 | 105 | 158 |
| | C_{33}^E | 389 | 211 | 267 |
| | C_{44}^E | 125 | 42 | 24 |

^aReferences 7, 8, and 11.

^bReferences 8 and 11.

^cReferences 9–11.

Now for the phonon propagation direction parallel to the z-axis, the electromechanical coupling constant from Eq. (14) reduces to

$$(K_{kl}(\bar{l}))^2 = \frac{1}{\epsilon_{\perp}} \begin{pmatrix} 0 & 0 & 0 & 0 & 0 & 0 \\ 0 & 0 & 0 & 0 & 0 & 0 \\ 0 & 0 & 0 & 0 & 0 & 0 \\ 0 & 0 & 0 & 0 & 0 & 0 \\ 0 & 0 & 0 & 0 & \frac{e_{z5}^2}{C_{44}^E} & 0 \\ 0 & 0 & 0 & 0 & 0 & 0 \end{pmatrix}. \quad (17)$$

Substituting the values of the respective coefficients from Table I, the change in elastic stiffness constant due to piezoelectric stiffening for the case of phonon propagation parallel to the z-axis for AlN is by 3%, for ZnO is by 7%, and for GaN 5%.

Now for the phonon propagation direction inclined at an angle 90° in the XZ plane, the electromechanical coupling constant from Eq. (14) reduces to

$$(K_{kl}(\bar{l}))^2 = \frac{1}{\epsilon'_{\parallel} C_{KL}^E} \begin{pmatrix} e_{z3}^2 & e_{z1}e_{z3} & e_{z1}e_{z3} & 0 & 0 & 0 \\ e_{z1}e_{z3} & e_{z1}^2 & e_{z1}^2 & 0 & 0 & 0 \\ e_{z1}e_{z3} & e_{z1}^2 & e_{z1}^2 & 0 & 0 & 0 \\ 0 & 0 & 0 & 0 & 0 & 0 \\ 0 & 0 & 0 & 0 & 0 & 0 \\ 0 & 0 & 0 & 0 & 0 & 0 \end{pmatrix}$$

and substituting the values of the respective coefficients from Table I the electromechanical coupling constant for AlN, ZnO, and GaN, respectively, reduces to

$$(K_{AlN})^2 = \begin{pmatrix} 0.08 & -0.12 & -0.12 & 0 & 0 & 0 \\ -0.12 & 0.01 & 0.03 & 0 & 0 & 0 \\ -0.12 & 0.03 & 0.01 & 0 & 0 & 0 \\ 0 & 0 & 0 & 0 & 0 & 0 \\ 0 & 0 & 0 & 0 & 0 & 0 \\ 0 & 0 & 0 & 0 & 0 & 0 \end{pmatrix},$$

$$(K_{ZnO})^2 = \begin{pmatrix} 0.09 & -0.08 & -0.08 & 0 & 0 & 0 \\ -0.08 & 0.02 & 0.02 & 0 & 0 & 0 \\ -0.08 & 0.02 & 0.02 & 0 & 0 & 0 \\ 0 & 0 & 0 & 0 & 0 & 0 \\ 0 & 0 & 0 & 0 & 0 & 0 \\ 0 & 0 & 0 & 0 & 0 & 0 \end{pmatrix},$$

$$(K_{GaN})^2 = \begin{pmatrix} 0.02 & -0.02 & -0.02 & 0 & 0 & 0 \\ -0.02 & 0.004 & 0.01 & 0 & 0 & 0 \\ -0.02 & 0.01 & 0.004 & 0 & 0 & 0 \\ 0 & 0 & 0 & 0 & 0 & 0 \\ 0 & 0 & 0 & 0 & 0 & 0 \\ 0 & 0 & 0 & 0 & 0 & 0 \end{pmatrix}.$$

Since the change in the elastic stiffness constants due to piezoelectric stiffening is $\leq 12\%$ for AlN, ZnO, and GaN, it is clear that useful results may be obtained without including stiffening effects. Accordingly, the results of the next section do not include the small corrections due to stiffening effects; this approximation makes it possible to obtain analytical results.

IV. RESULTS AND DISCUSSION

There has been significant amount of research on energy harvesting from piezoelectric stack coupled in shoe sole during rapid locomotion and cantilever based piezoelectric generators using piezoceramic and polymeric materials.^{12,13} In all these applications, the strain is applied vertically along the z-axis (c-axis) of the nanowire or bent at an angle with respect to the z-axis.

Now considering the first case where the strain is applied along the z-axis (stretched/compressed along the c-axis) of the nanowire, $\frac{\partial u_z}{\partial z}$ is the dominant component of the strain. Neglecting the strain components in all other directions, the piezoelectrically induced polarization from Eq. (7) reduces to

$$P_{rzz} = e'_{x3} \cos \phi \frac{\partial u_z}{\partial z} = (-e_{z1} \sin^3 \eta - e_{z3} \cos^2 \eta \sin \eta + e_{x5} \cos \eta \sin 2\eta) \cos \phi \frac{\partial u_z}{\partial z}, \quad (18a)$$

$$P_{\phi zz} = -e'_{x3} \sin \phi \frac{\partial u_z}{\partial z} = (-e_{z1} \sin^3 \eta - e_{z3} \cos^2 \eta \sin \eta + e_{x5} \cos \eta \sin 2\eta) \sin \phi \frac{\partial u_z}{\partial z}, \quad (18b)$$

$$P_{zzz} = e'_{z3} \frac{\partial u_z}{\partial z} = (e_{z1} \cos \eta \sin^2 \eta + e_{z3} \cos^3 \eta + e_{x5} \sin \eta \sin 2\eta) \frac{\partial u_z}{\partial z}. \quad (18c)$$

Therefore, the piezoelectric potential generated across the nanowire for $\frac{\partial u_z}{\partial z}$ being the only non-zero strain is

$$\begin{aligned}
 V_{zz} &= -\frac{1}{\epsilon'' - \epsilon_0} \int \bar{\mathbf{P}} \cdot d\bar{\rho} \\
 &= -\frac{1}{\epsilon'' - \epsilon_0} \left[\int P_{rzz} dr + \int r P_{\phi zz} d\phi + \int P_{zzz} dz \right].
 \end{aligned} \quad (19)$$

The piezoelectric potential distribution as a function of strain applied along z-axis for 50 nm thick and 600 nm long (a) AlN (b) ZnO, and (c) GaN nanowire for phonon propagation along z-axis is shown in Fig. 1. On stretching the nanowire such that there is 0.1% strain along z-axis, the piezoelectric voltage generated across the AlN nanowire is -15.1 V, for ZnO nanowire is -11.3 V, and for GaN is -4.9 V.

Figure 2 shows the piezoelectric potential distribution as a function of strain applied along z-axis for 50 nm thick and 600 nm long (a) AlN (b) ZnO, and (c) GaN nanowire for the phonon propagation at an angle 45° in the XZ plane. In this case, the magnitude as well as the polarity of the piezoelectric voltage generated exhibits a polar dependence. The maximum potential observed across the AlN nanowire is 2.8 V, across the ZnO nanowire is 3.7 V, and across the GaN nanowire is 2 V.

Figure 3 shows the piezoelectric potential distribution as a function of strain applied along z-axis for 50 nm thick and 600 nm long (a) AlN (b) ZnO, and (c) GaN nanowire for phonon propagation at an angle 90° in the XZ plane, i.e., either parallel to x-axis or parallel to y-axis. In this case also, the potential generated varied from positive to negative and back to positive over ϕ and the maximum voltage observed is 3 V for AlN nanowire, 2.6 V for ZnO nanowire, and 1.2 V for GaN nanowire.

Now considering the cantilever approach, $\frac{\partial u_r}{\partial z}$ is the dominant component of strain. Neglecting the strain components in all other directions, cylindrical polar components of the

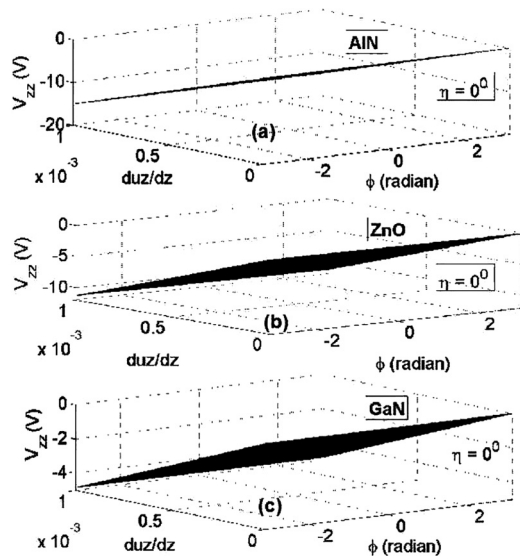


FIG. 1. Piezoelectric potential distribution as a function of strain applied along z-axis for 50 nm thick and 600 nm long (a) AlN (b) ZnO, and (c) GaN nanowire. The phonon propagation direction is parallel to z-axis.

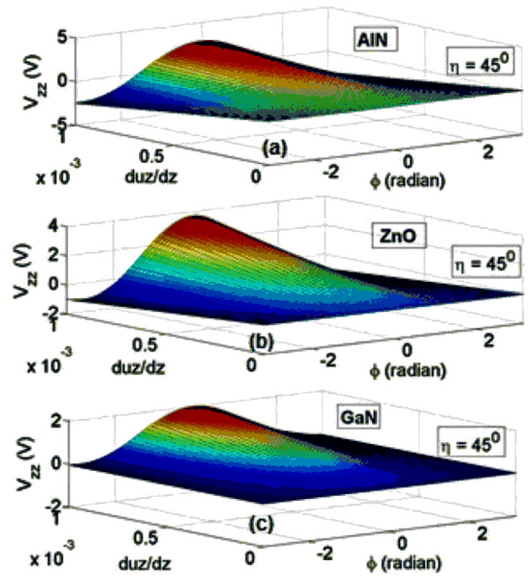


FIG. 2. (Color online) Piezoelectric potential distribution as a function of strain applied along z-axis for 50 nm thick and 600 nm long (a) AlN (b) ZnO, and (c) GaN nanowire. The phonon propagation direction is inclined at 45° in the XZ plane.

piezoelectrically induced polarization from Eq. (7) reduces to

$$\begin{aligned}
 P_{rrz} &= (e'_{y4} \sin^2 \phi + e'_{x5} \cos^2 \phi) \frac{\partial u_r}{\partial z} \\
 &= \left(e_{x5} \cos \eta \sin^2 \phi + \left(-e_{z1} \frac{\sin \eta \sin 2\eta}{2} \right. \right. \\
 &\quad \left. \left. + e_{z3} \frac{\sin \eta \sin 2\eta}{2} + e_{x5} \cos \eta \cos 2\eta \right) \right. \\
 &\quad \left. \cos^2 \phi \right) \frac{\partial u_r}{\partial z},
 \end{aligned} \quad (20a)$$

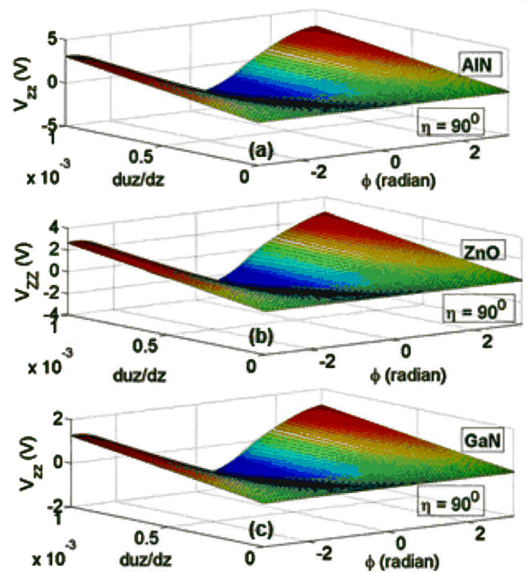


FIG. 3. (Color online) Piezoelectric potential distribution as a function of strain applied along z-axis for 50 nm thick and 600 nm long (a) AlN (b) ZnO, and (c) GaN nanowire. The phonon propagation direction is inclined at 90° in the XZ plane.

$$\begin{aligned}
 P_{\phi rz} &= (e'_{y4} \sin \phi \cos \phi + e'_{x5} \sin \phi \cos \phi) \frac{\partial u_r}{\partial z} \\
 &= \left(e_{x5} \cos \eta \frac{\sin 2\phi}{2} - \left(-e_{z1} \frac{\sin \eta \sin 2\eta}{2} \right. \right. \\
 &\quad \left. \left. + e_{z3} \frac{\sin \eta \sin 2\eta}{2} + e_{x5} \cos \eta \cos 2\eta \right) \right) \frac{\sin 2\phi}{2} \frac{\partial u_r}{\partial z}, \quad (20b)
 \end{aligned}$$

$$\begin{aligned}
 P_{zrz} &= e'_{z5} \cos \phi \frac{\partial u_r}{\partial z} \\
 &= \left(e_{z1} \frac{\cos \eta \sin 2\eta}{2} - e_{z3} \frac{\cos \eta \sin 2\eta}{2} \right. \\
 &\quad \left. + e_{x5} \sin \eta \cos 2\eta \right) \cos \phi \frac{\partial u_r}{\partial z}. \quad (20c)
 \end{aligned}$$

Therefore, the piezoelectric potential generated across the nanowire for $\frac{\partial u_r}{\partial z}$ being the only non-zero strain is

$$\begin{aligned}
 V_{rz} &= -\frac{1}{\epsilon'' - \epsilon_0} \int \bar{P} \cdot d\bar{\rho} \\
 &= -\frac{1}{\epsilon'' - \epsilon_0} \left[\int P_{rrz} dr + \int r P_{\phi rz} d\phi \right. \\
 &\quad \left. + \int P_{zrz} dz \right]. \quad (21)
 \end{aligned}$$

The piezoelectric potential distribution as a function of strain applied radially for 50 nm thick and 600 nm long (a) AlN (b) ZnO, and (c) GaN nanowire for phonon propagation along the z-axis is shown in Fig. 4. On bending the nanowire such that there is a 0.1% strain developed along z-axis, the piezoelectric voltage generated across the AlN nanowire is 0.41 V, for ZnO nanowire is 0.41 V, and for GaN is 0.21 V.

Figure 5 shows the piezoelectric potential distribution as a function of strain applied radially for 50 nm thick and 600

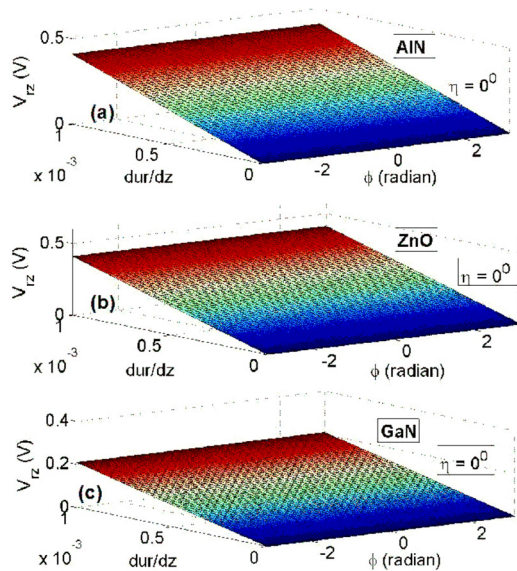


FIG. 4. (Color online) Piezoelectric potential distribution as a function of strain applied radially for 50 nm thick and 600 nm long (a) AlN (b) ZnO, and (c) GaN nanowire. The phonon propagation direction is parallel to the z-axis.

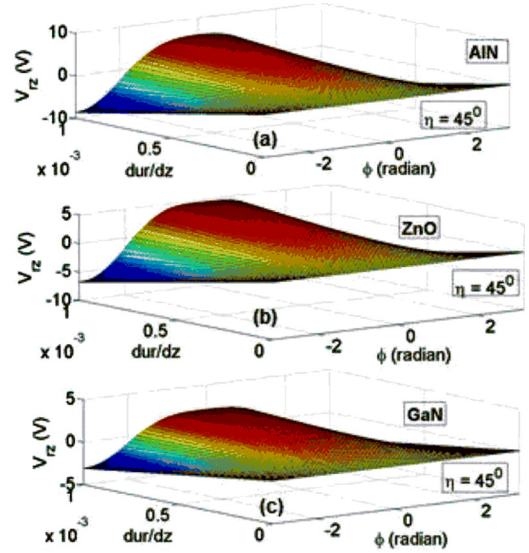


FIG. 5. (Color online) Piezoelectric potential distribution as a function of strain applied along z-axis for 50 nm thick and 600 nm long (a) AlN (b) ZnO, and (c) GaN nanowire. The phonon propagation direction is inclined at 45° in the XZ plane.

nm long (a) AlN (b) ZnO, and (c) GaN nanowire for the phonon propagation at an angle 45° in the XZ plane. In this case, the magnitude as well as the polarity of the piezoelectric voltage generated exhibits a polar dependence. The maximum potential observed across the AlN nanowire is 6 V, across the ZnO nanowire is 4.5 V, and across the GaN nanowire is 2.1 V.

Figure 6 shows the piezoelectric potential distribution as a function of strain applied radially for 50 nm thick and 600

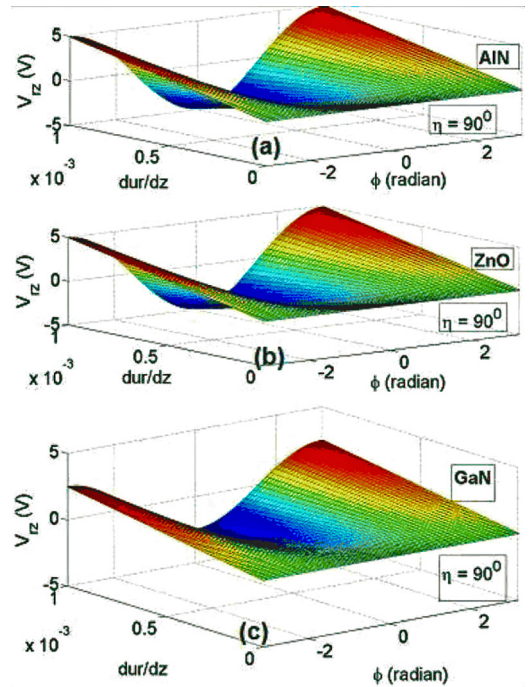


FIG. 6. (Color online) Piezoelectric potential distribution as a function of strain applied along z-axis for 50 nm thick and 600 nm long (a) AlN (b) ZnO and (c) GaN nanowire. The phonon propagation direction is inclined at 90° in the XZ plane.

nm long (a) AlN (b) ZnO, and (c) GaN nanowire for phonon propagation at an angle 90° in the XZ plane, i.e., either parallel to x-axis or parallel to y-axis. In this case also, the potential generated varied from positive to negative back to positive over ϕ and the maximum voltage observed is 4.9 V for AlN nanowire, 4.9 V for ZnO nanowire, and 2.5 V for GaN nanowire. In this paper we have estimated the piezoelectrically induced electric potential distribution in AlN, ZnO, and GaN nanowires for the zero free-charge case. This (order of magnitude) is in agreement with the experimental results reported by Wang's group for ZnO nanowires.¹⁴ With the presence of free charge in the nanowires, there will be electron-phonon as well as hole-phonon interactions and the net output voltage generated will be affected by this phonon scattering as proposed by Alexe's group.¹⁵ The importance of the effect produced by this non-zero density of free charge will depend on the specific details of each nanowire piezo generator, such as the contact geometry, the contact materials, the doping of the nanowire, the mobility of the nanowire, and the self-consistent fields in the nanowire; accordingly, these effects are beyond the scope of this present treatment. Indeed, in this treatment, the primary emphasis has been placed on the piezo effects existing in the nanowires of cylindrical geometry as reflected by the use of cylindrical coordinates throughout the formulation.

V. CONCLUSION

The piezoelectrically induced electric polarization vector and the associated potential have been derived in terms of the acoustic phonon mode amplitude displacement for

wurtzite nanowires. In this treatment, the semiconductors have been modeled for the case of no free charge. By comparing generated piezoelectric potentials for strains applied in specific directions in these nanowires, it is shown that the maximum piezo energy is generated for the vertical direction (i.e., along z-axis). In terms of energy generation, AlN and ZnO nanowires are found to be superior to GaN nanowires. In order to obtain analytic results, piezoelectric stiffening has been neglected since the change in elastic constants for these semiconductor nanowires is only a few percent.

¹C. Sun, J. Shi, and X. Wang, *J. Appl. Phys.* **108**, 034309 (2010).

²L. C. Lew Yan Voon and M. Willatzen, *J. Appl. Phys.* **109**, 031101 (2011).

³J. Song, J. Zhou, and Z. L. Wang, *Nano Lett.* **6**, 1656 (2006).

⁴K. Momeni, G. M. Odegard, and R. S. Yassara, *J. Appl. Phys.* **108**, 114303 (2010).

⁵B. A. Auld, *Acoustic Fields and Waves in Solids* (Wiley, New York, 1973).

⁶M. Strosio and K. W. Kim, *Phys. Rev. B* **48**, 1936 (1993).

⁷C. Persson, R. Ahuja, A. Ferreira da Silva, and B. Johansson, *J. Crystal Growth* **231**, 407 (2001).

⁸H. Morkoç and U. Ozgur, *Zinc Oxide: Fundamentals, Materials and Device Technology* (Wiley, New York, 2009).

⁹H. Morkoç, *Handbook of Nitride Semiconductors and Devices*, Materials Properties, and Growth, Vol. 1 (Wiley, New York, 2008).

¹⁰V. Bougrov, M. E. Levinshtein, S. L. Rumyantsev, and A. Zubrilov, *Properties of Advanced Semiconductor Materials GaN, AlN, InN, BN, SiC, SiGe* (Wiley, New York, 2001).

¹¹T. Hanada, *Oxide and Nitride Semiconductors*, Advances in Material Research, Vol. 12 (Springer, Berlin, 2009).

¹²J. A. Paradisco and T. Starner, *Pervasive Comput.* **4**, 18 (2005).

¹³S. P. Beeby, M. J. Tudor, and N. M. White, *Meas. Sci. Technol.* **17**, R175 (2006).

¹⁴Z. H. Wang, *Adv. Mater.* **21**, 1311 (2009).

¹⁵M. Alexe, S. Senz, M. A. Schubert, D. Hesse, and U. Gosele, *Adv. Mater.* **20**, 4021 (2008).